Bratislava Medical Journal
https://doi.org/10.1007/s44411-026-00490-9

RESEARCH

Bee Bread Shows Protective Effects in a Streptozotocin-Induced Alzheimer's Disease Rat Model

Alev Duygu Acun[1] · Ebru Afşar[2] · Deniz Kantar[1]

Received: 1 August 2025 / Revised: 29 August 2025 / Accepted: 7 January 2026
© The Author(s) 2026

Abstract

Alzheimer's disease (AD) is currently a global concern, and treating its current symptoms and slowing its progression is an important goal. To this end, identifying biochemical mechanisms that have the potential to prevent and improve the pathology of the disease is a priority. The response of the central nervous system to pathological insults may be neuroinflammation. Kynurenine (KYN) pathway metabolites, which are closely related to neuroinflammation, may have the potential to affect many neural processes such as synaptic plasticity, neurotransmission, antioxidant mechanisms, and neurogenesis. In addition, it has been recently shown that there is a strong correlation between sensory system deterioration and AD progression and that neuropathological changes in sensory regions can be detected before changes in memory-related regions. For this purpose, our study aimed to investigate the effects of changes in the Kynurenine (KYN) pathway on cognitive functions and auditory sensory system functions in an experimental AD model and the effects of bee bread (BB), known to have anti-inflammatory properties, on these parameters. It was shown that BB has the potential to improve memory by exerting a healing effect on neuroinflammation, apoptosis, and the KYN pathway, and also has a therapeutic effect on auditory sensory system functions, reducing sensory system integrity disorders. These results highlight the ability of BB to prevent neurotoxic effects associated with sAD. It may be a potential protector as a food supplement for AD neuropathological health, and further studies are needed for this purpose.

✉ Deniz Kantar
dkantar@akdeniz.edu.tr

[1] Faculty of Medicine, Akdeniz University, Arapsuyu, 07070 Antalya, Turkey

[2] Faculty of Dentistry, Kapadokya University, Esbelli, 50400 Nevsehir, Turkey

Published online: 20 January 2026

Graphical Abstract

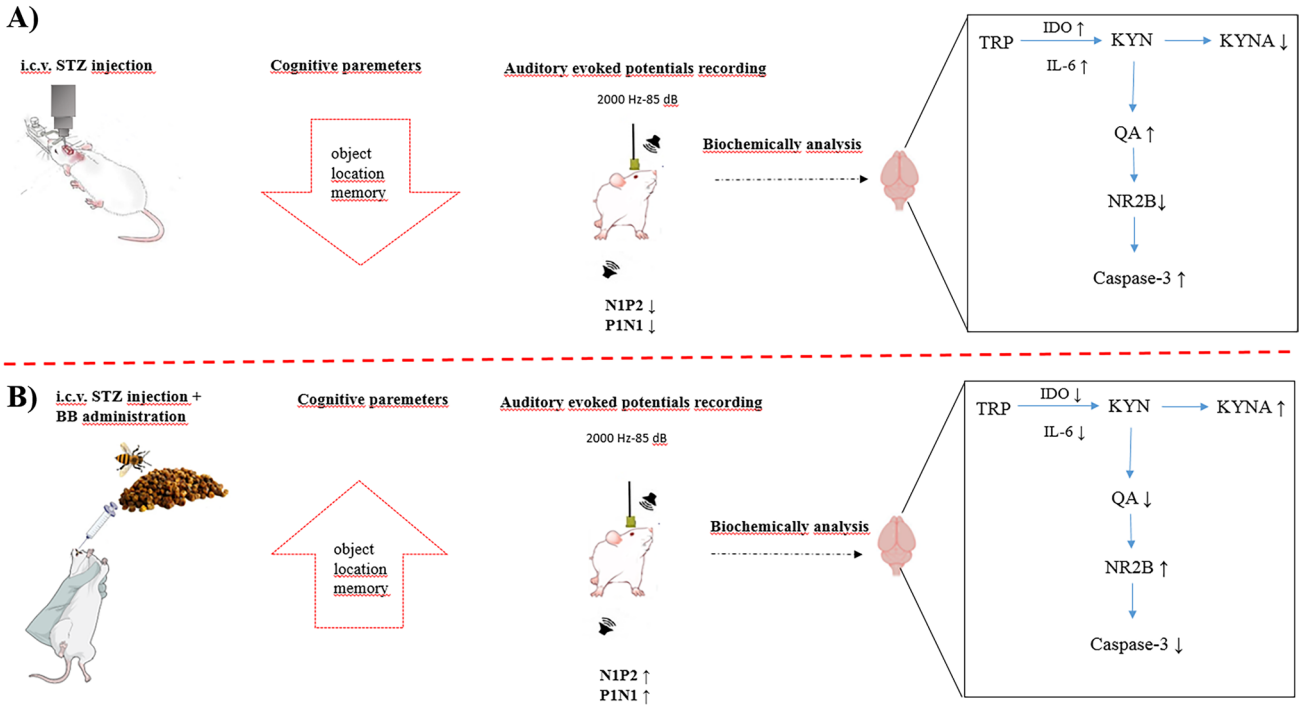

Keywords Alzheimer's disease · Kynurenine pathway · Bee bread · Object location test · Auditory evoked potentials

Abbreviations

AD	Alzheimer's disease
Aβ	Amyloid-beta
ICV	Intracerebroventricular
OD	Optical density
AEP	Auditory evoked potential
ERP	Event-related potentials
EP	Evoked potentials
KYN	Kynurenine
TRP	Tryptophan
TDO	Tryptophan 2,3-dioxygenase
IDO	Indolamine 2,3-dioxygenase
QA	Quinolinic acid
NMDA	N-methyl-D-aspartate
NMDAR	N-methyl-D-aspartate receptor
KYNA	Kynurenic Acid
BB	Bee Bread
STZ	Streptozotocin
sAD	Sporadic Alzheimer'a disease
ISI	Interstimulus ınterval
i.p.	Intraperitoneal
HRP	Horseradish peroxidase
IL-6	Interleukin-6

1 Introduction

Alzheimer's disease (AD), which accounts for 60–70% of cases worldwide, is a progressive neurodegenerative disease that damages nerve cells and ultimately leads to the death of the patient. Brain tissue atrophies due to damage to neural cells, resulting in loss of neurotransmission and synaptic activity between various cortical regions. In the early stages of AD, some researchers accept that there is more widespread atrophy, especially in auditory structures, and auditory dysfunction [1]. Although it is generally observed that auditory-evoked potentials in the cerebral cortex are reduced in patients with AD or in animal models, there are conflicting results in the literature [2]. Therefore, the effect of AD on auditory-evoked potentials and their dynamic changes in the development of the disease remain unclear [3]. Neuropathological changes may begin in sensory areas before AD pathology manifests in memory areas, and neuropathological changes may occur in sensory-related areas before cognitive symptoms become evident [4]. While AD can cause hearing loss, hearing loss can also accelerate the development of AD [5]. Auditory evoked potentials (AEPs) are electrical potentials in any part of the auditory system, from the cochlea to the cerebral cortex, evoked by an auditory stimulus. AEPs are a non-invasive method used to obtain information about

the function and integrity of the auditory system [6]. Since AEP does not include cognitive processing and perception patterns, it may be more effective than event-related potentials (ERPs) in evaluating changes in the auditory network. The early components of the AEP are considered suitable for cross-species studies because they represent automatic brain functions that involve auditory discrimination without consciousness [7]. Rodent AD models are very important because they allow the investigation of the direct relationship between AD neuropathology and its neurophysiological effects on brain neural networks. However, there are few studies in the literature using evoked potentials (EPs)/ERPs paradigms in rodent AD models [8]. Although changes in AEP responses have been studied in some AD animal models [9, 10], the dynamic changes of AEP in the development of AD have still not been fully elucidated.

Neuroinflammation is known to play a critical role in the development of AD. The release of proinflammatory cytokines may cause synaptic dysfunction, neuronal death, and inhibition of neurogenesis, and is likely to be linked to AD. Neuroinflammation is closely linked to the kynurenine (KYN) pathway and underlies various neurological conditions. This link is due to the ability of inflammatory factors to affect the activity of enzymes involved in the KYN pathway. The KYN pathway involves the conversion of the essential amino acid tryptophan (Trp) into a series of compounds and is considered an important metabolic pathway as some of the compounds formed are neuroactive [11]. The KYN pathway and its several metabolites are thought to be altered in AD and to have significant roles in the neuropathogenesis of the disease. Variations in KYN metabolites have an impact on the brain's ability to regulate oxidative stress, cause neuroinflammation, and cause neurotoxicity. Therefore, any imbalance in the metabolism of the KYN pathway may play an important role in AD pathophysiology [12]. In order to evaluate the systemic and metabolic defects in AD pathophysiology, in-depth study of the KYN pathway is crucial.

In the KYN pathway, TRP 2,3-dioxygenase (TDO) and indolamine 2,3-dioxygenase (IDO) are known to be the initial rate-limiting enzymes. Although TDO is the main enzyme under physiological conditions, IDO1 is upregulated in macrophages, microglia, neurons, and astrocytes in response to neuroinflammatory stimuli. Proinflammatory cytokines released by microglia activate the IDO enzyme, which raises the neurotoxic quinolinic acid (QA) level. The neuroactive QA metabolite has N-methyl-D-aspartate (NMDA) receptor (NMDAR) agonist characteristics and is a potent producer of free radicals. Additionally, through raising extracellular glutamate levels, it produces excitotoxicity and triggers lipid peroxidation. When anti-inflammatory cytokines are released from astrocytes, the synthesis of kynurenic acid (KYNA), a potent NMDAR antagonist, is increased. KYNA exhibits competitive antagonistic activity on NMDA receptors. Overactivation of the KYN pathway may lead to overproduction of QA, and QA has been found to be associated with pathological changes and cognitive functions in AD. QA has been observed to cause learning and memory deficits. A vicious loop may be created whereby overproduction of QA causes greater tau hyperphosphorylation, which in turn triggers activation of microglia in response to Aβ and p-tau. Although it is widely accepted that AD is associated with an elevated KYN pathway, further research is needed to explore the elusive molecular mechanisms behind the relationship between AD and metabolites of the complex KYN pathway and to develop therapeutic strategies for this [12].

Recently, complementary and herbal medicine has gained popularity and interest. Bee bread (BB) is a natural product formed by anaerobic lactic fermentation of bee pollen. Although BB contains less protein than bee pollen, the digestibility of the protein it contains is higher due to the fermentation of the collected pollen by the bees [13]. This makes BB a functional food source with higher bioavailability compared to bee pollen [14]. Properties such as high concentration of simple sugar content, low pH (pH 4), low water activity, high oxidation–reduction potential and the presence of lactic acid bacteria make bee bread a preservative composition [15]. BB is an important source of antioxidants that can eliminate free oxygen radicals and their harmful effects on cells [16]. Since TRP is known to be an important compound in the content of BB [13], it is likely to modulate the KYN pathway. According to a study, propolis extracts suppress IDO activity as part of their immunomodulatory effects [17]. A high Trp diet has also been previously shown to significantly improve cognitive dysfunction and reduce Aβ deposits [18]. Therefore, although it seems plausible that BB regulates the KYN pathway and reduces TRP degradation, its therapeutic effects on AD remain unclear.

Intracerebroventricular (ICV) administration of streptozotocin (STZ), a glucosamine-nitrosourea molecule derived from soil bacteria, mimics the neuropathological and metabolic changes of sporadic AD (sAD) [19, 20]. The ICV-STZ model is widely used to mimic the onset and course of human sAD and to investigate the neuroprotective effects of different drugs [21]. This study investigated the effects of BB treatment applied to the ICV-STZ sAD model on the level of KYN pathway metabolites and their anti-apoptotic, anti-inflammatory, cognitive functions, changes in sensory brain responses and anti-Alzheimer potential.

2 Materials and Methods

2.1 Animals and Treatment

Forty male albino Wistar rats, 3 months old, weighing 250–300 g, were obtained from Akdeniz University Animal Care Unit (Antalya, Turkey) and housed in groups of 4 in stainless steel cages under standard conditions (23 ± 1 °C and 50 ± 5% humidity) with a 12-h light–dark cycle. Food and water were provided ad libitum. Animals were randomly divided into three groups (n = 6 each group): (1) Sham (SH) group [vehicle (citrate buffer/2 µl/ventricle) plus water gavage treatment]; (2) STZ group [STZ (2 mg/kg, 2 µl/ventricle) plus water gavage treatment]; (3) STZB group [STZ (2 mg/kg, 2 µl/ventricle) plus BB (200 mg/kg/day) gavage treatment]. Studies have reported that 2 mg/kg is the most effective STZ dose in modeling sporadic AD-like pathology [22, 23]. The purity of STZ (Cayman, 13,104), whose molecular formula is C8H15N3O7, is over 95%. To prepare an STZ solution corresponding to a dose of 2 mg/kg for a rat weighing 350 g, 1.05 mg of STZ should be diluted in 6 µl of citrate buffer (0.05 M). The 0.05 M citrate buffer solution was prepared according to the procedures given previously [22]. Since the half-life of the STZ solution is very short (15–30 min) and unstable, it was prepared fresh before use. After the surgical procedure, the animals were allowed to recover for seven days and then gavage was applied once a day for 21 days. The nutritional content of BB purchased from Nutral Therapy Company (Erciyes University Technopark, Kayseri) is given in the table (Table 1). In previous studies, 200 mg/kg/day bee bread application was preferred because it is known to have positive effects on the number of apoptotic cells, weight control and other parameters [24].

Table 1 Nutritional contents of BB

Nutritional elements	Content
Ash	2.31 g / 100 g
Protein	22.63g / 100 g (N×6.25)
Carbohydrate	51.91 g / 100 g
Dietary fiber	18.18 g / 100 g
Fat (acid hydrolyzed)	8.70 g / 100 g
Energy	376 kcal / 100 g
Gluten (ppm)	-
Copper (Cu)	12.91 mg / kg
Zinc (Zn)	36.67 mg / kg
Phosphorus (P)	6665.44 mg / kg
İron (Fe)	192 mg / kg
Calcium (Ca)	1390 mg / kg
Sodium (Na)	78.74 mg / kg
Magnesium (Mg)	638 mg / kg
Omega-6	0.23 g / 100 g
Omega-3	0.55 g / 100 g
Humidity	14.45 g / 100 g
Total antioxidant activity	447.16 mg TE / 100 g

2.2 Experimental Design

The ICV-STZ sAD rat model was established as in previous studies [22, 23]. Under ketamine (80 mg/kg, i.p.)/xylazine (5 mg/kg, i.p.) anesthesia, rats were placed in a standard stereotaxic apparatus and a midsagittal incision was made in the scalp. The lateral ventricles (AP: -0.8 mm, ML: ± 1.4 mm, DV: -4.0 mm) were drilled bilaterally using a dental drill. 0.5 µl/min was injected for 5 min with a Hamilton syringe. After surgery, the incision was sutured, and antibiotic ointment was applied for 7 days to prevent infection. Penicillin (40,000 U) was injected intramuscularly daily for 3 days. After waiting for a 7-day period for AD pathology to occur, gavage was applied for 21 days. Since significant cognitive impairment and neurodegeneration are known to occur approximately 30 days after 2 mg/kg ICV-STZ injection [25–27], the training phase of the behavioral experiment was performed on day 29, and the testing phase on day 30. After electrode placement and recordings for electrophysiological recording on day 31, rats were sacrificed. Perfusion was performed with isotonic heparin via cardiac cannula and then brain tissues were removed and frozen in liquid nitrogen. Brain tissues were stored at -80 °C for biochemical analyses (Fig. 1).

2.3 AEP Recordings and Analysis

To record auditory electrophysiological responses, rats were anesthetized with urethane (1.2 g/kg, i.p. Sigma-Aldrich, St Louis, MO, USA) and fixed in a standard stereotaxic frame. Active electrodes were placed in holes drilled in the auditory cortices of the rats (AP: -4.5 mm, ml: -3.5 and + 3.5 mm), while reference/ground stainless steel screw electrodes were placed bilaterally over the cerebellar region. Before recording, the tympanic membrane and external auditory canal were checked for any damage. Tones of 50 ms duration were delivered to the rat's ear via a loudspeaker 15 cm away. The signal was amplified (Brainamp EEG/EP Amplifier, Brain Products, Munich, Germany), band-pass filtered (0.1–300 Hz, 50 Hz notch filter), and digitized and recorded at a sampling rate of 1000 Hz (Brainvision Recorder, Brain Products, Munich, Germany). Using tones at 2000 Hz that were 85 dB and had a 500 ms short interstimulus interval (ISI), AEPs were recorded. The BrainVision Analyzer

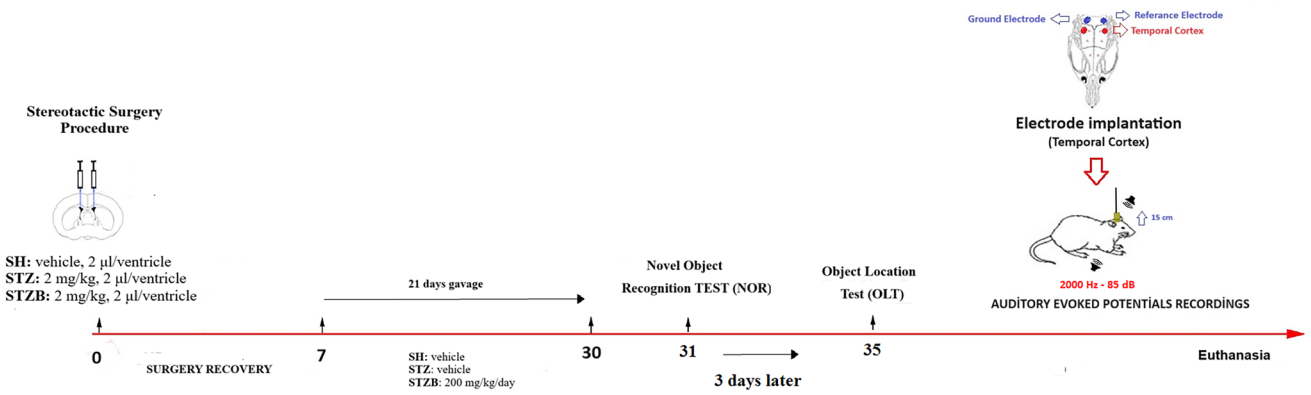

Fig. 1 A schematic flow chart of the material-method diagram

(Brain Products, Munich, Germany) was used to average the EEG data. AEPs were divided into 600 ms epochs, 100 ms before and 500 ms after stimulus presentation. The average of 100 AEP waves was used to identify the peaks, and the resulting waveforms were used to calculate the peak-to-peak amplitudes (in microvolts) of the AEP components for each rat. The first large positive wave that appeared approximately 50 ms after the stimulus was defined as P1. Similarly, the large negative wave that appeared approximately 100 ms was determined as N1 and the positive wave that appeared at 200 ms was determined as P2. The peak-to-peak amplitudes of P1N1 and N1P2 were analyzed according to the measurements.

2.4 Behavioral Testing

Both experiments were conducted in a soundproof room in a box system measuring 40 cm × 40 cm × 40 cm, with uniform lighting, and covered with a white mat on the bottom and sides. Both tests consisted of two phases: a training phase and a test phase. Each object used in the experiment was fixed to the floor to prevent movement. Before each trial for each rat, the objects and the entire interior of the box were wiped with 70% ethanol to prevent the presence of olfactory cues and air-dried. The rats' behavior during the training and test phases was recorded with a video camera. Video recordings were used to determine the time the rats spent with the objects, and the rat was considered to have explored the object when its nose was 2 cm away from the object.

2.5 Object Location Test (OLT)

In the training phase, two identical objects, A1 and A2, were selected and placed on opposite sides of the box, and the rat was left in the center of the box and given 5 min to explore objects A1 and A2. In the testing phase, 24 h after the training phase, two identical objects, A1, remained in the same place as in the training phase, while the other identical object, A2, was placed in a new location to test object location memory. The discrimination index was calculated using the following formula: Exploration time spent with an object in the new location/Exploration time spent with an object in the new location + Exploration time spent with an object in the old location × 100.

2.5.1 Novel Object Recognition (NOR) Test

During the training phase, two identical objects (A1-A2) were placed in the experimental system at two opposite positions at the same distance from the nearest corner. The rats were then released from the center to the field and allowed 5 min to explore these two identical objects (A1-A2). The rats that completed the training phase were taken to the test phase 24 h after they were placed back in their cages. To test the novel object recognition memory during the test phase, a copy of the familiar object (A3) and a new object (B1) were placed in the same place as during the training experiment. In the novel object recognition test, discrimination index (%) values showing memory strength were analyzed. Discrimination index was calculated using the formula: exploration time spent with novel object/ exploration time spent with novel object + exploration time spent with familiar object × 100.

2.6 Biochemical Experiments

Temporal and hippocampal tissue samples homogenized in cold PBS, centrifuged at 2000–3000 r.p.m for 20 min. Supernatants were stored at − 80 °C for protein analyses.

The sandwich ELISA method is very effective in detecting the target antigen in an unknown sample. Temporal and hippocampal target protein levels in the supernatants of tissue homogenates were measured according to the procedures of a commercially available sandwich ELISA

kit. Commercial kits contain 96-well plates coated with rat target protein antibodies, and biotinylated rat target protein antibody is added to these wells, which bind to the target protein in the sample. A sandwich model is created by adding a horseradish peroxidase (HRP) conjugate polyclonal antibody specific for target protein to obtain immobilized target protein. Then, streptavidin-HRP is added to bind to the biotinylated target protein antibody. After incubation, unbound components are removed by washing 5 times and then substrate solution is added. When the substrate solution is added, HRP reacts with the enzyme to cause color formation, so only the wells containing target protein show a color change proportional to the amount of target protein. Then, an acidic solution is added to terminate the reaction and the optical density (OD) is measured spectrophotometrically at 450 nm. Sample target protein amount was also calculated from the standard curve plot.

Target Proteins: Total Aβ1-42 (SunRedBio Rat Aβ1-42 Catalog No: 201–11-0094), Tau protein (SunRedBio Rat Tau Protein Catalog No. SRB-T-86822), glutamate receptor2B (NR2B/NMDAR2B (SunRedBio Rat NR2B Protein Catalog No: 201–11-2688), TRP (SunRedBio Rat TRP Protein Catalog No: 201–11-7308), KYN (SunRedBio Rat KYN Catalog No: 201–11-2152), KYNA (SunRedBio Rat KYNA Catalog No. 201–11-5219), QA (SunRedBio Rat QA Protein Catalog No: 201–11-5093), Caspase-3/CPP32 (SunRedBio Rat Caspase-3 Catalog No: 201–11-0281), interleukin 6 (IL-6) (SunRedBio Rat IL-6 Catalog No: 201–11-0136).

2.7 Statistical analysis

Statistical analyses were performed using SPSS 23.0 for Windows (SPSS, Chicago, IL, USA) program. Statistical comparisons of the data obtained from biochemical analyses between groups were performed using one-way ANOVA and post-hoc Tukey test for data conforming to normal distribution. AEP analyses were performed using repeated-measures ANOVA and post-hoc comparisons were made using the Bonferroni test. Results were given as mean ± standard error and $p < 0.05$ was considered significant.

3 Results

3.1 Treatment with BB Ameliorates Cognitive İmpairment in STZ-induced AD Rats

In the OLT test, the novelty feature is the location, since the objects in the test trial are the same as in the training trial. The OLT is considered a simple and effective test that measures hippocampus-dependent spatial memory. When OLT was examined 24 h after training, it requires de novo transcription and translation [28]. A statistically significant difference was found between the groups in OLT test [F(2,15) = 46,16, $p < 0.001$, N = 18] (Fig. 2A). The OLT discrimination index of the STZ group (45,23 ± 1,5) decreased significantly compared to the SH group (78,68 ± 2,51) ($p < 0.001$). The OLT discrimination index of the STZB group (76,73 ± 3,78) increased significantly compared to the STZ group ($p < 0.001$). No significant difference was found between the SH and STZB groups.

The major advantage of the NOR over other rodent memory tests is that it relies on rodents' natural tendency to explore novelty. Several different brain regions are critical for the new object recognition memory, including the insular cortex, the perirhinal cortex, and the ventromedial prefrontal cortex [29]. A statistically significant difference was found between the groups in NOR test [F(2,15) = 39,37, $p < 0.001$, N = 18] (Fig. 2B). The NOR discrimination index of the STZ group (49,96 ± 2,2) decreased significantly compared to the SH group (79,13 ± 2,4) ($p < 0.001$). The NOR discrimination index of the STZB group (74,69 ± 2,8) increased significantly ($p < 0.001$) compared to the STZ group. No significant difference was found between the SH and STZB groups. Therefore, it was observed that long-term spatial memory of STZ-induced AD group rats was impaired, while BB treatment had an improving effect on memory functions.

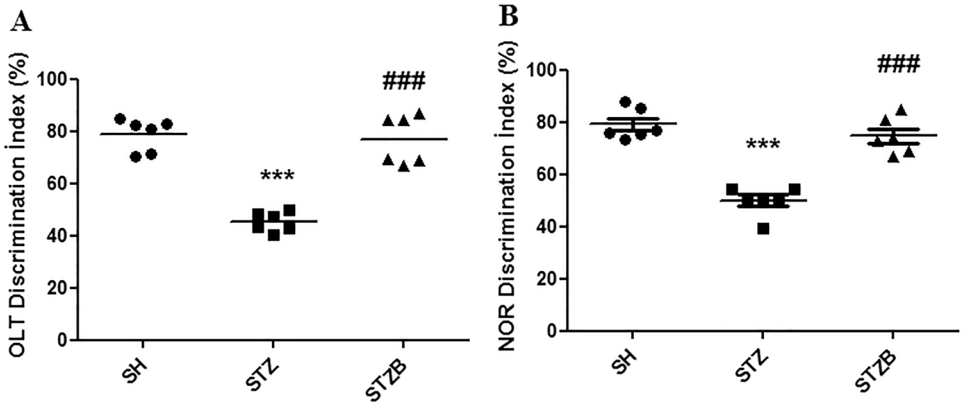

Fig. 2 A The object location memory discrimination index B: The correlations between OLT discrimination index and hippocampus IL-6 levels, C: The correlations between OLT discrimination index and hippocampus NR2B levels. Results are presented as mean ± SEM. (*: Significant vs SH group, #: Significant vs STZ group, *: $p < 0.05$; **: $p < 0.01$; ***: $p < 0.001$, #: $p < 0.05$; ##: $p < 0.01$; ###: $p < 0.001$)

3.2 While STZ Induction Increases Alzheimer-like Pathology, BB has an Ameliorating Effect on this Pathology

Data from thousands of studies on the pathophysiology of AD to date identify Aβ and tau protein as key players [30]. Statistically significant difference was found between the hippocampus Aβ1-42 levels between the groups [F(2,15) = 3,48, $p < 0.05$, N = 18] (Fig. 3A). Hippocampal Aβ1-42 levels of the STZ group (26,32 ± 2.27 pg/mg) tended to increase, although not significantly, compared to the SH group (22,35 ± 1,3 pg/mg) (p > 0.05). Hippocampus Aβ1-42 levels of the STZB group (19,68 ± 1,6 pg/mg) were found to be significantly decreased compared to the STZ group ($p < 0.05$). There was a statistically significant difference in temporal Aβ1-42 levels between groups [F(2,15) = 30,65, $p < 0.001$, N = 18] (Fig. 3B). Temporal Aβ1-42 levels of the STZ group (28,16 ± 1,2 pg/mg) were significantly higher than those of the SH group (16,85 ± 1,4 pg/mg) ($p < 0.01$). It was observed that temporal Aβ1-42 levels of the STZB group (14,33 ± 1,2 pg/mg) were significantly decreased compared to the STZ group ($p < 0.001$).

No statistically significant difference was found between the hippocampus tau levels between the groups [F(2,15) = 0,56, $p < 0.05$, N = 18] (Fig. 3C). Hippocampal Tau levels in the STZ group (2,21 ± 0,33 ng/mg) were significantly higher than in the SH group (1,28 ± 0,16 ng/mg) ($p < 0.05$). Hippocampal Tau levels of the STZB group (1,84 ± 0,22 ng/mg) tended to decrease compared to the STZ group (p > 0.05). There was a statistically significant difference in temporal tau levels between groups [F(2,15) = 11,39, $p < 0.01$, N = 18] (Fig. 3D). Temporal Tau levels of the STZ group (3,29 ± 0,3 ng/mg) were significantly higher than those of the SH group (1,24 ± 0,2 ng/mg) ($p < 0.01$). Temporal Tau levels of the STZB group (2,21 ± 0,3 ng/mg) tended to decrease compared to the STZ group (p > 0.05). In summary, these results indicate that Aβ and Tau pathology occur in the hippocampus and temporal cortex of STZ-induced AD rats and that BB treatment may alleviate the neuronal damage that may arise due to these.

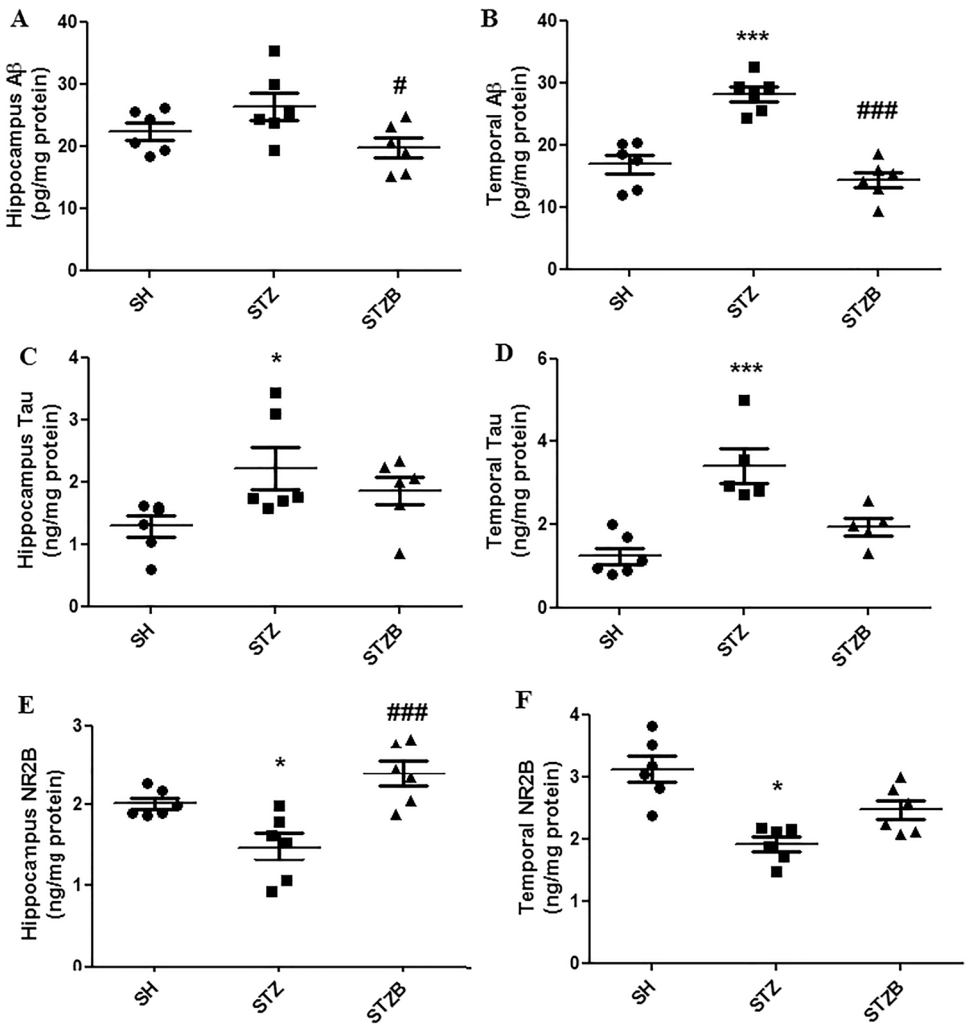

Fig. 3 A: Hippocampus Aβ levels, B: Temporal Aβ levels, C: Hippocampus Tau levels, D: Temporal Tau levels. N = 6 in all experimental groups. E: Hippocampus NR2B levels, F: Temporal NR2B levels. Results are presented as mean ± SEM. (*: Significant vs SH group, #: Significant vs STZ group, *: $p < 0.05$; **: $p < 0.01$; ***: $p < 0.001$, #: $p < 0.05$; ##: $p < 0.01$; ###: $p < 0.001$)

3.3 BB Treatment İncreased Glutamate Receptor-2B/NR2B/NMDAR2B Levels in the Hippocampal Regions of STZ-İnduced AD rats

NR2B activation may be associated with the pathological progression of AD. Furthermore, the detrimental effects of Aβ prior to neuronal loss appear to be mediated by NMDARs, particularly NR2Bs [31]. There was a statistically significant difference in hippocampus NR2B levels between groups [F(2,15) = 10,63, $p < 0.001$, N = 18] (Fig. 3E). Hippocampus NR2B levels of the STZ group (1,48 ± 0,1 ng/mg) were significantly higher than those of the SH group (2,01 ± 0,06 ng/mg) ($p < 0.05$). Hippocampus NR2B levels of the STZB group (2,38 ± 0,1 ng/mg) were significantly increased compared to the STZ group ($p < 0.001$). No significant difference was found in hippocampal NR2B levels of the STZB group compared to the SH group ($p > 0.05$). There was a statistically significant difference in temporal NR2B levels between groups [F(2,15) = 13,58, $p < 0.001$, N = 6] (Fig. 3F). Temporal NR2B levels of the STZ group (1,91 ± 0,11 ng/mg) were significantly lower than those of the SH group (3,11 ± 0,2 ng/mg) ($p < 0.001$). Temporal NR2B levels of the STZB group (2,46 ± 0,15 ng/mg) were tented to increase compared to the STZ group ($p < 0.05$). While increased apoptosis was observed in the STZ-induced rat group, it was significantly decreased especially in the hippocampal regions due to BB treatment.

3.4 Attenuating Effect of BB Treatment on Increased Proinflammatory IL-6 Levels in STZ-induced AD Rats

Chronic neuroinflammation, induced by a series of proinflammatory cytokines such as IL-6, is widely accepted as an early and persistent feature of the AD brain [32, 33]. There was a statistically significant difference in hippocampus IL-6 levels between groups [F(2,15) = 11,46, $p < 0.01$, N = 18] (Fig. 4A). Hippocampus IL-6 levels of the STZ group (26,42 ± 2,11 pg/mg) were significantly higher than those of the SH group (16,55 ± 1,03 pg/mg) ($p < 0.01$). Hippocampus IL-6 levels of the STZB group (18,53 ± 2,4 pg/mg) were significantly lower than the STZ group ($p < 0.05$). There was a statistically significant difference in temporal IL-6 levels between groups [F(2,15) = 5,74, $p < 0.01$, N = 6] (Fig. 4B). Temporal IL-6 levels of the STZ group (34,95 ± 6,2 pg/mg) were significantly higher than those of the SH group (14,94 ± 2,95 pg/mg) ($p < 0.01$). Temporal IL-6 levels of the STZB group (19,6 ± 3,1 pg/mg) were significantly lower than the STZ group ($p > 0.05$). Increased IL-6 levels were observed in the temporal cortex and hippocampal brain regions of STZ-induced AD rats, while BB treatment was particularly effective in reducing hippocampal neuroinflammation.

3.5 Apoptotic Marker Caspase-3 Decreased in STZ-Induced AD Rats Due to BB Treatment

There was a statistically significant difference in hippocampus caspase-3 levels between groups [F(2,15) = 11,46,

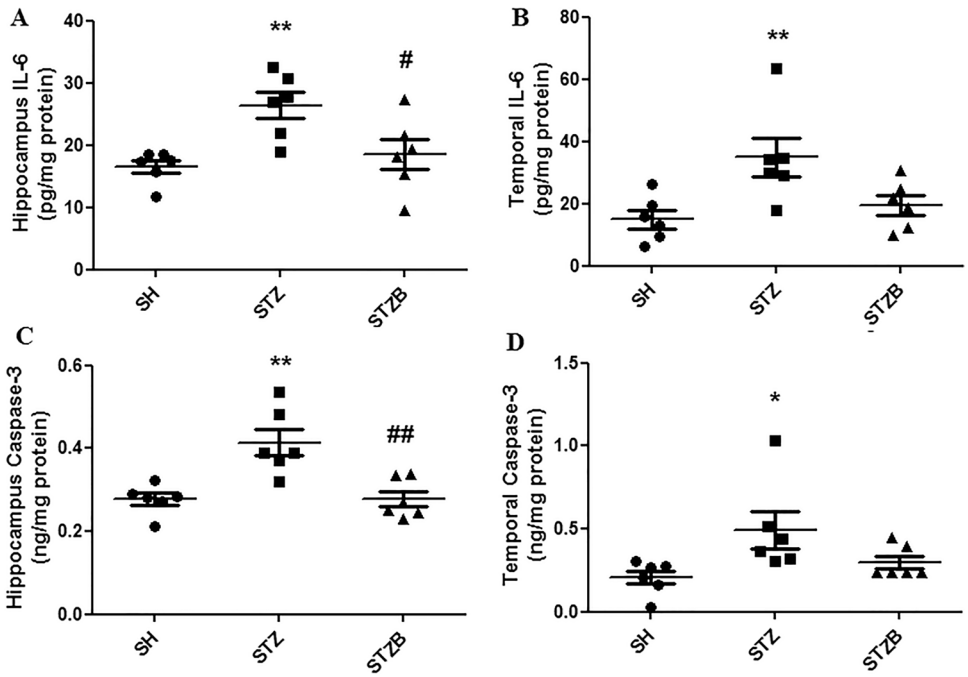

Fig. 4 A: Hippocampus IL-6 levels, B: Temporal IL-6 levels, C: Hippocampus Caspase-3 levels, D: Temporal Caspase-3 levels. N = 6 in all experimental groups. Results are presented as mean ± SEM. (*: Significant vs SH group, #: Significant vs STZ group, *: $p < 0.05$; **: $p < 0.01$; ***: $p < 0.001$, #: $p < 0.05$; ##: $p < 0.01$; ###: $p < 0.001$)

$p < 0.001$, N = 18] (Fig. 4C). Hippocampus caspase-3 levels of the STZ group (0,41 ± 0,03 ng/mg) were significantly higher than those of the SH group (0,27 ± 0,01 ng/mg) ($p < 0.01$). Hippocampus caspase-3 levels in the STZB group (0.27 ± 0.01 ng/mg) were significantly lower than those in the STZ group ($p < 0.01$). No significant difference was found in temporal caspase levels of the STZB group compared to the SH group (p > 0.05). There was a statistically significant difference in temporal caspase-3 levels between groups [F(2,15) = 4,13, $p < 0.05$, N = 18] (Fig. 4D). Temporal caspase-3 levels of the STZ group (0,49 ± 0,11 ng/mg) were significantly higher than those of the SH group (0,20 ± 0,04 ng/mg) ($p < 0.05$). Temporal caspase levels of the STZB group (0.29 ± 0.03 ng/mg) were tented to decrease compared to the STZ group (p > 0.05). No significant difference was found in temporal caspase levels of the STZB group compared to the SH group (p > 0.05). While increased apoptosis was observed in the STZ-induced rat group, it was significantly decreased, especially in the hippocampal regions, due to BB treatment.

3.6 Neuroprotective Effect of BB on the KYN Pathway in STZ-Induced Rats

All data of the KYN pathway are presented in Table 2. Statistically significant difference was found in hippocampus KYN levels between the groups [F(2,15) = 3,98, $p < 0.05$, N = 18]. Hippocampus KYN levels of the STZ group were higher than those of the SH group ($p < 0.05$). Hippocampus KYN levels of the STZB group tended to decrease compared to the STZ group (p > 0.05). There was a statistically significant difference in temporal KYN levels between groups [F(2,15) = 7,41, $p < 0.01$, N = 18]. Temporal KYN levels of the STZ group were higher than those of the SH group ($p < 0.05$). Temporal KYN levels of the STZB group were significantly decreased compared to the STZ group ($p < 0.01$). No statistically significant difference was found in hippocampus TRP levels between the groups [F(2,15) = 2,20, p > 0.05, N = 18]. There was a no statistically significant difference in temporal TRP levels between groups [F(3,20) = 5,35, p > 0.05, N = 18]. There was no statistically significant difference in hippocampus KYN/TRP ratios between groups [F(2,15) = 3,07, p > 0.05, N = 18]. There was no statistically significant difference in temporal KYN/TRP ratios between groups [F(2,15) = 3,34, p > 0.05, N = 18]. The change in the KYN/TRP ratio is a ratio used to determine IDO activity by reflecting the degradation rate of TRP [34]. There was a statistically significant difference in hippocampus KYNA levels between groups [F(2,15) = 5,82, $p < 0.05$, N = 18]. Hippocampus KYNA levels of the STZ group were significantly lower than the SH group ($p < 0.05$). Hippocampus KYNA levels of the STZB group were significantly increased compared to those of the STZ group ($p < 0.05$). There was a statistically significant difference in temporal KYNA levels between groups [F(2,15) = 9,04, $p < 0.01$, N = 18]. Temporal KYNA levels of the STZ group were significantly lower than the SH group ($p < 0.01$). Temporal KYNA levels of the STZB group were significantly higher than the STZ group ($p < 0.05$). There was a statistically significant difference in hippocampal QA levels between groups [F(2,15) = 9,48, $p < 0.01$, N = 18]. Hippocampal QA levels of the STZ group were significantly higher than the SH group ($p < 0.01$). Hippocampal QA levels of the STZB group tended to decrease compared to the STZ group (p > 0.05). No significant difference was found in hippocampal QA levels of the STZB group compared to the SH group (p > 0.05). There was a statistically

Table 2 Changes in the KYN pathway and its metabolites in the hippocampus and temporal brain regions. Results are presented as mean ± SEM. (*: Significant vs SH group, #: Significant vs STZ group, *: $p < 0.05$; **: $p < 0.01$; ***: $p < 0.001$, #: $p < 0.05$; ##: $p < 0.01$; ###: $p < 0.001$)

	HİPPOCAMPUS	TEMPORAL CORTEX
KYN (ng/mg protein)	SH	1.68 ± 0.26
	2.26 ± 0.25	
	STZ	2.68 ± 0.26 *
	3.64 ± 0.45 *	
	STZB	2.06 ± 0.22
	2.10 ± 0.13 ##	
TRP (ng/mg protein)	SH	1.64 ± 0.23
	2.73 ± 0.23	
	STZ	1.67 ± 0.23
	2.92 ± 0.34	
	STZB	2.27 ± 0.23
	2.59 ± 0.47	
KYN/TRP Ratio	SH	
	1.72 ± 0.31	0.85 ± 0.11
	STZ	
	1.75 ± 0.26	1.30 ± 0.16
	STZB	
	0.92 ± 0.009	0.91 ± 0.11
KYNA (nmol/mg protein)	SH	
	1.40 ± 0.22	1.68 ± 0.21
	STZ	
	0.54 ± 0.13 *	0.55 ± 0.16 **
	STZB	
	1.24 ± 0.20 #	1.52 ± 0.22 #
QA (ng/mg protein)	SH	
	0.09 ± 0001	0.13 ± 0.02
	STZ	
	0.16 ± 0.01 **	0.26 ± 0.04 **
	STZB	
	0.12 ± 0.01	0.14 ± 0.01 #

significant difference in temporal QA levels between groups [F(2,15) = 6,54, $p < 0.01$, N = 18]. Temporal QA levels of the STZ group were significantly higher than the SH group ($p < 0.01$). Temporal QA levels of the STZB group were significantly lower than the STZ group ($p < 0.05$). No significant difference was found in temporal QA levels of the STZB group compared to the SH group ($p > 0.05$). In the STZ-induced AD group, it was found that while excitotoxin KYN pathway metabolites increased, the number of neuroprotective metabolites decreased significantly and the TRP pathway shifted towards QA production. However, BB treatment results were found to reverse these results observed in STZ rats and direct the KYN pathway towards neuroprotective KYNA production.

3.7 Peak-to-Peak Amplitudes in AEP Responses İncreased due to BB Treatment

Recently, sensory system deficits, including auditory systems, have been found to be highly associated with AD progression, and impairments in sensory-related areas may occur before AD pathology becomes evident. Hearing loss due to AD pathology may occur, which may accelerate the development of AD and dementia [3]. In all experimental groups, peak-to-peak amplitude values of AEP components were measured over one negative (N1) and two positive potentials (P2) seen at the temporal left (T3) electrode region. P1N1 amplitude value was found to differ significantly between the groups [F(2,15) = 7,90, $p < 0.01$, N = 18]. P1N1 peak-to-peak amplitude value of STZ group (6.49 ± 1.03 µV) was found to decrease significantly compared to SH group (12.40 ± 0.96 µV) ($p < 0.01$). N1P1 peak-to-peak amplitude value of STZB group (9.43 ± 1.14 µV) tended to increase compared to STZ group, while there was no significant difference with SH group ($p > 0.05$) (Fig. 5A). N1P2 amplitude value was found to differ significantly between the groups [F(2,15) = 23.62, $p < 0.001$, N = 18]. It was found that the N1P2 peak-to-peak amplitude value of the STZ group (2,40 ± 0,54 µV) was significantly decreased compared to the SH group (11.50 ± 1.35 µV) ($p < 0.05$). The N1P2 peak-to-peak amplitude value of the STZB group (2.40 ± 0.54 µV) tended to increase compared to the STZ group, while no significant difference was found compared to the SH group ($p > 0.05$) (Fig. 5B). The decreases in peak-to-peak amplitude values of STZ-induced AD rats reflect sensory system integrity (Fig. 5C). This may occur due to decreased neuronal density or firing desynchronization. It has been observed that BB treatment may have a healing effect on the sensory system, especially by increasing the N1P2 amplitude, which is related to the processing and interpretation of auditory information.

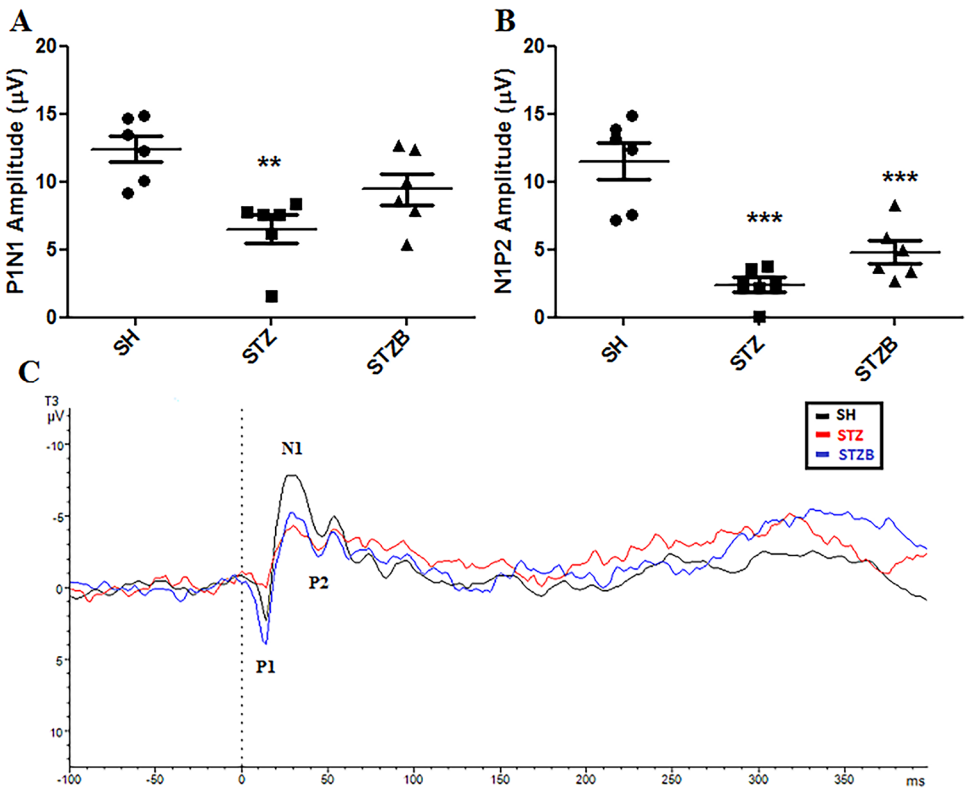

Fig. 5 A: Averages of peak-to-peak amplitudes of the P1N1 AEP component, B: Averages of peak-to-peak amplitudes of the N1P2 AEP component. C: Representative shape of AEP waveforms evoked by auditory stimuli at the Left Temporal (T3) electrode location. Results are presented as mean ± SEM. (*: Significant vs SH group, #: Significant vs STZ group, *: $p < 0.05$; **: $p < 0.01$; ***: $p < 0.001$, #: $p < 0.05$; ##: $p < 0.01$; ###: $p < 0.001$)

3.8 Correlations of OLT Discrimination Index with Hippocampus IL-6 and NR2B

Pearson correlation analysis was used to evaluate all correlation analysis. As a result of the analysis, a negative relationship was found between OLT discrimination index and changes in hippocampus IL-6 levels (Pearson r = -0.667, $p < 0.01$, N = 18) (Fig. 6A). According to the results of the correlation analysis, it can be concluded that there is a significant decrease in OLT discrimination index due to the increase in hippocampus IL-6 levels. As a result of the analysis, a positive relationship was found between OLT discrimination index and changes in hippocampus NR2B levels (Pearson r = 0,592, $p < 0.01$, N = 18) (Fig. 6B). According to the results of the correlation analysis, it can be concluded that there was a significant increase in the OLT discrimination index due to the increase in hippocampal NR2B levels.

4 DİSCUSSİON

The aim of our study was to examine changes in the KYN molecular pathway, long-term memory, and electrophysiological responses in the ICV-STZ sAD model and the possible neuroprotective effects of BB against ICV-STZ-induced AD. The pathological changes induced by ICV injection of STZ resemble the features of sAD [22]. Studies have shown that a 2 mg/kg ICV-STZ dose causes significant cognitive impairment and neurodegeneration approximately 30 days after injection [22, 25–27].

Indeed, the results of our study showed that the OLT and NOR discrimination index of the STZ group decreased significantly compared to the SH group, indicating long-term memory impairment. The OLT assesses spatial learning that relies mainly on hippocampal activity, whereas the NOR reflects nonspatial learning of object identity that relies on multiple brain regions [35]. In the hippocampal tissue, IL-6 levels were significantly increased in the STZ group compared to SH, and a negative correlation was found between the OLT discrimination index and hippocampal IL-6 levels. Chronic neuroinflammation induced by IL-6 is widely accepted to be an early and persistent feature of the AD brain [32, 33] and is assumed to be responsible for the development of cognitive impairment seen in AD [36]. In line with this, our findings suggest that hippocampal inflammation may underlie the impaired spatial memory performance.

KYN pathway activation was also evident in the hippocampus. Although TRP levels and KYN/TRP ratios did not change significantly, KYN, QA, caspase-3, and Tau levels were significantly increased, while KYNA levels were significantly decreased in the STZ rats compared to the SH group. The overactivated KYN pathway may lead to overproduction of the excitotoxin QA via microglia activation [12]. QA, known to overstimulate NR2B-containing NMDARs, is associated with excitotoxicity, apoptosis, and Aβ pathology [12, 37–40]. It is known that QA also induces apoptosis in astrocytes and is closely related to the formation of Aβ and p-tau in the brain [37]. These results suggest that QA-mediated hippocampal neuronal damage and apoptosis may contribute to the deterioration in memory performance. Conversely, KYNA, a neuroprotective metabolite with antioxidant and anti-inflammatory effects [41–43], was found to be decreased, further supporting a mechanism promoting excitotoxicity and cognitive decline. These results suggest that hippocampal neuronal damage and apoptosis mediated by QA may contribute to impaired memory performance.

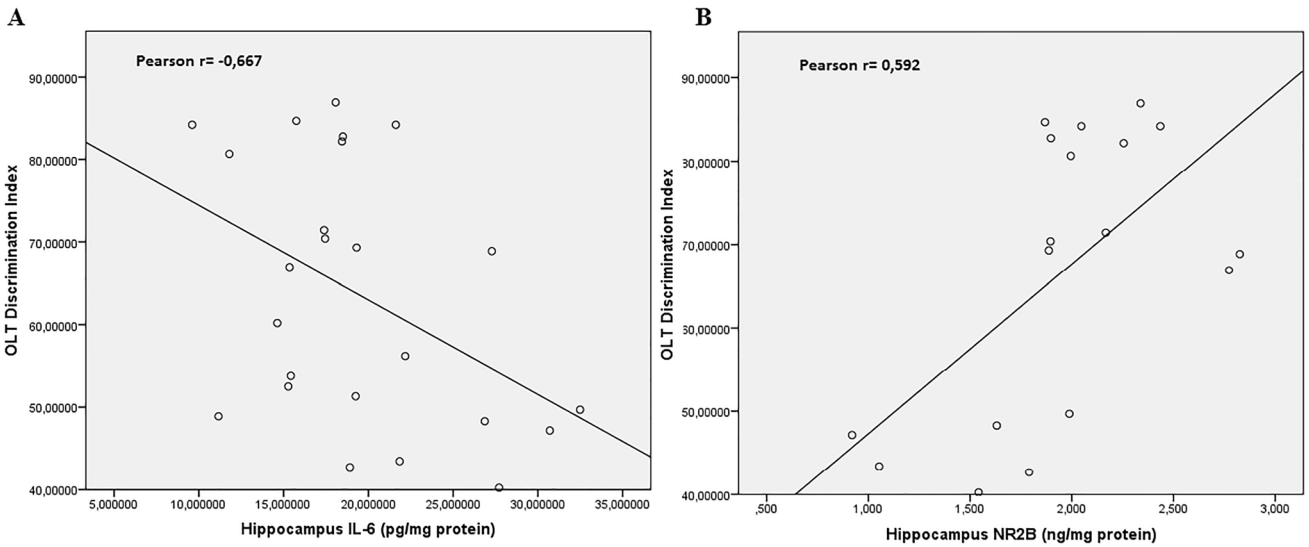

Fig. 6 A: The object location memory discrimination index B: The correlations between OLT discrimination index and hippocampus IL-6 levels

Therefore, increased QA levels due to inflammation are likely to damage neurons in brain regions through NMDARs, impairing learning and memory, as well as synaptic plasticity, KYNA is known as one of the neuroprotective metabolites of the KYN pathway, which can antagonize excitatory neurotoxicity through NMDAR-mediated antagonism and has antioxidant effects [41].

BB is essential because it is a natural product with high nutritional and medicinal value [44]. In addition, it is known to be the most powerful antioxidant bee product. Inflammation is a common underlying cause of serious diseases because it initiates a pathogenic cascade such as metabolic pathway failure, tissue damage and even necrosis and apoptosis [45]. BB treatment exerted a protective effect on hippocampal pathology. In the STZB group, hippocampal IL-6 and caspase-3 levels were significantly reduced compared to the STZ group and were comparable to the SH group. Moreover, the OLT discrimination index was significantly higher in the STZB group, indicating improved hippocampal-dependent spatial memory. In addition, hippocampal NR2B levels were positively correlated with OLT performance, consistent with previous findings suggesting NR2B contributes to enhanced synaptic plasticity and memory [46, 47]. These results indicate that BB can ameliorate hippocampal neuroinflammation and apoptosis, thereby improving cognitive functions.

Alongside memory functions, electrophysiological measures from the temporal cortex also showed significant alterations. Sensory system deteriorations are reported to precede cognitive symptoms in AD [4, 48, 49], and auditory evoked potentials (AEPs) provide a window into these early changes. In our study, temporal cortex analyses showed that both P1N1 and N1P2 amplitudes were significantly decreased in the STZ group compared to SH, reflecting impaired sensory processing. Since the initial AEP waveforms (P1N1, N1P2) mainly represent sensory responses within the auditory and temporal cortices [3, 50], these findings indicate disruption of auditory network integrity in the sAD model. The observed reductions in amplitude may result from desynchronization of neuronal firing or decreased neuronal density in the temporal cortex, both of which are sensitive to early AD-related degeneration.

Importantly, BB treatment improved electrophysiological responses in the temporal cortex. The N1P2 peak-to-peak amplitude was significantly increased in STZB rats compared to STZ rats, and P1N1 amplitude also tended to improve. These findings suggest that BB has the potential to restore auditory sensory processing and that AEP measures may serve as useful biomarkers for monitoring both early disease progression and therapeutic efficacy.

Furthermore, temporal cortex molecular results paralleled electrophysiological findings. In STZ rats, KYN and QA levels were significantly increased, along with elevated Aβ1-42 and NR2B, while KYNA levels were decreased compared to SH. BB treatment reversed these alterations by reducing KYN, QA, Aβ1-42, and NR2B levels while increasing KYNA in the temporal cortex. This suggests that BB not only modulates hippocampal-dependent cognitive processes but also exerts protective effects on temporal cortical networks, thereby normalizing both molecular and electrophysiological responses.

Taken together, our results demonstrate that the ICV-STZ model reproduces hippocampal-dependent memory impairment and temporal cortex sensory dysfunction observed in sAD. BB exerts protective effects in both regions by reducing neuroinflammation, modulating KYN pathway metabolites, and normalizing neuronal activity. These dual improvements in hippocampal memory functions and temporal cortex electrophysiological responses highlight the potential of BB as a therapeutic agent against AD-related pathology.

Studies have shown that there are gender differences in the AD model induced by ICV-STZ. In general, it has been determined that female rats induced by ICV-STZ are more resistant to ICV-STZ damage and that there are gender differences in brain responses to expected changes. This finding clearly contradicts the knowledge that female rats are prone to AD disease [51]. However, female rats are generally not preferred in STZ studies because it is thought that they may be resistant to the neurodegenerative effects of STZ due to hormonal oscillations of the estral cycle [52]. In order to minimize this limitation, we also used male rats in our study. Despite the limitations of this experimental model, the results of our study suggest that the ICV-STZ model may be suitable for examining the contribution of AD pathology and electrophysiological changes.

Acknowledgements Not applicable.

Author Contributions A.D.A. and D.K. generated the rat models. E.A. analyzed ELISA's data. A.D.A. wrote the main manuscript text and prepared figures and table. A.D.A, E.A. and D.K. were involved in data interpretation, critically reviewed and provided their final approval of the manuscript, and agreed to be accountable for the work.

Funding Open access funding provided by the Scientific and Technological Research Council of Türkiye (TÜBİTAK). This study was not supported by any funding.

Data Availability No datasets were generated or analysed during the current study.

Declarations

Conflict of interest The authors declare no competing interests.

Ethical Approval Ethical approval for this work was obtained from Akdeniz University Local Committee on Animal Research Ethics (ethics approval ID: 1656/2023.12.001).

Clinical trial number Not applicable.

Consent to Participate Not applicable.

Consent for Publication Not applicable.

Open Access This article is licensed under a Creative Commons Attribution 4.0 International License, which permits use, sharing, adaptation, distribution and reproduction in any medium or format, as long as you give appropriate credit to the original author(s) and the source, provide a link to the Creative Commons licence, and indicate if changes were made. The images or other third party material in this article are included in the article's Creative Commons licence, unless indicated otherwise in a credit line to the material. If material is not included in the article's Creative Commons licence and your intended use is not permitted by statutory regulation or exceeds the permitted use, you will need to obtain permission directly from the copyright holder. To view a copy of this licence, visit http://creativecommons.org/licenses/by/4.0/.

References

1. Swords GM, Nguyen LT, Mudar RA, Llano DA. Auditory system dysfunction in Alzheimer disease and its prodromal states: a review. Ageing Res Rev. 2018;44:49–59.
2. Gurevicius K, Lipponen A, Tanila H. Increased cortical and thalamic excitability in freely moving APPswe/PS1dE9 mice modeling epileptic activity associated with Alzheimer's disease. Cereb Cortex. 2013;23(5):1148–58.
3. Mei L, Liu LM, Chen K, Zhao HB. Early functional and cognitive declines measured by auditory-evoked cortical potentials in mice with Alzheimer's disease. Front Aging Neurosci. 2021;13:710317.
4. Murphy C. Olfactory and other sensory impairments in Alzheimer disease. Nat Rev Neurol. 2019;15(1):11–24.
5. Morrison C, Rabipour S, Knoefel F, Sheppard C, Taler V. Auditory event-related potentials in mild cognitive impairment and Alzheimer's disease. Curr Alzheimer Res. 2018;15(8):702–15.
6. Ignatious E, Azam S, Jonkman M, De Boer F. Frequency and time domain analysis of EEG based auditory evoked potentials to detect binaural hearing in noise. J Clin Med. 2023. https://doi.org/10.3390/jcm12134487.
7. Kim B, Shin J, Kim Y, Choi JH. Destruction of ERP responses to deviance in an auditory oddball paradigm in amyloid infusion mice with memory deficits. PLoS ONE. 2020;15(3):e0230277.
8. Babiloni C, Blinowska K, Bonanni L, Cichocki A, De Haan W, Del Percio C, et al. What electrophysiology tells us about Alzheimer's disease: a window into the synchronization and connectivity of brain neurons. Neurobiol Aging. 2020;85:58–73.
9. Wang J, Ikonen S, Gurevicius K, Van Groen T, Tanila H. Altered auditory-evoked potentials in mice carrying mutated human amyloid precursor protein and presenilin-1 transgenes. Neuroscience. 2003;116(2):511–7.
10. Stoiljkovic M, Kelley C, Stutz B, Horvath TL, Hajos M. Altered cortical and hippocampal excitability in TgF344-AD rats modeling Alzheimer's disease pathology. Cereb Cortex. 2019;29(6):2716–27.
11. Cortes Malagon EM, Lopez Ornelas A, Olvera Gomez I, Bonilla Delgado J. The kynurenine pathway, aryl hydrocarbon receptor, and Alzheimer's disease. Brain Sci. 2024. https://doi.org/10.3390/brainsci14090950.
12. Liang Y, Xie S, He Y, Xu M, Qiao X, Zhu Y, et al. Kynurenine pathway metabolites as biomarkers in Alzheimer's disease. Dis Markers. 2022;2022:9484217.
13. Bakour M, Laaroussi H, Ousaaid D, El Ghouizi A, Es-Safi I, Mechchate H, et al. Bee bread as a promising source of bioactive molecules and functional properties: an up-to-date review. Antibiotics. 2022. https://doi.org/10.3390/antibiotics11020203.
14. de Giovanini Oliveira Sartori A, Martelli Chaib Saliba AS, Seneda Martarello N, Goldoni Lazarini J, Pedroso Gomes do Amaral JE, da Fernandes Pinto Luz C, et al. Changes in phenolic profile and anti-inflammatory activity of *Baccharis* beebread during gastrointestinal digestion/intestinal permeability in vitro. Food Chem. 2024;432:137234.
15. Staroň M, Alkassab AT, Sabo R, Demková L, Valenčáková A, Michalko M, et al. Higher early than late-season residue load of pesticides in honey bee bread in Slovakia. Apidologie. 2024;55(4):41.
16. Clarkson PM, Thompson HS. Antioxidants: what role do they play in physical activity and health? Am J Clin Nutr. 2000;72(2 Suppl):637S-646S.
17. Girgin G, Baydar T, Ledochowski M, Schennach H, Bolukbasi DN, Sorkun K, et al. Immunomodulatory effects of Turkish propolis: changes in neopterin release and tryptophan degradation. Immunobiology. 2009;214(2):129–34.
18. Pan S, Zhang Y, Ye T, Kong Y, Cui X, Yuan S, et al. A high-tryptophan diet alleviated cognitive impairment and neuroinflammation in APP/PS1 mice through activating aryl hydrocarbon receptor via the regulation of gut microbiota. Mol Nutr Food Res. 2024;68(2):e2300601.
19. Grieb P. Intracerebroventricular streptozotocin injections as a model of Alzheimer's disease: in search of a relevant mechanism. Mol Neurobiol. 2016;53(3):1741–52.
20. Plaschke K, Kopitz J, Siegelin M, Schliebs R, Salkovic-Petrisic M, Riederer P, et al. Insulin-resistant brain state after intracerebroventricular streptozotocin injection exacerbates Alzheimer-like changes in Tg2576 AbetaPP-overexpressing mice. J Alzheimers Dis. 2010;19(2):691–704.
21. Kraska A, Santin MD, Dorieux O, Joseph-Mathurin N, Bourrin E, Petit F, et al. In vivo cross-sectional characterization of cerebral alterations induced by intracerebroventricular administration of streptozotocin. PLoS ONE. 2012;7(9):e46196.
22. Moreira-Silva D, Vizin RCL, Martins TMS, Ferreira TL, Almeida MC, Carrettiero DC. Intracerebral injection of streptozotocin to model Alzheimer disease in rats. Bio Protoc. 2019;9(20):e3397.
23. Dehghan-Shasaltaneh M, Naghdi N, Choopani S, Alizadeh L, Bolouri B, Masoudi-Nejad A, et al. Determination of the best concentration of streptozotocin to create a diabetic brain using histological techniques. J Mol Neurosci. 2016;59(1):24–35.
24. Doganyigit Z, Yakan B, Soylu M, Kaymak E, Okan A, Silici S. Histological, immunohistochemical and biochemical effects of bee bread on stomach tissue of obese rats. Bratisl Lek Listy. 2020;121(7):504–11.
25. Moreira-Silva D, Carrettiero DC, Oliveira ASA, Rodrigues S, Dos Santos-Lopes J, Canas PM, et al. Anandamide effects in a streptozotocin-induced Alzheimer's disease-like sporadic dementia in rats. Front Neurosci. 2018;12:653.
26. Motzko-Soares ACP, Vizin RCL, Martins TMS, Hungaro ARO, Sato JR, Almeida MC, et al. Thermoregulatory profile of neurodegeneration-induced dementia of the Alzheimer's type using intracerebroventricular streptozotocin in rats. Acta Physiol (Oxf). 2018;224(2):e13084.
27. Vicente MC, Almeida MC, Bicego KC, Carrettiero DC, Gargaglioni LH. Hypercapnic and hypoxic respiratory response during wakefulness and sleep in a streptozotocin model of Alzheimer's disease in rats. J Alzheimers Dis. 2018;65(4):1159–74.
28. Lima RH, Rossato JI, Furini CR, Bevilaqua LR, Izquierdo I, Cammarota M. Infusion of protein synthesis inhibitors in the entorhinal cortex blocks consolidation but not reconsolidation of object recognition memory. Neurobiol Learn Mem. 2009;91(4):466–72.

29. Acun AD, Kantar D, Er H, Erkan O, Derin N, Yargicoglu P. Investigation of cyclo-Z therapeutic effect on insulin pathway in Alzheimer's rat model: biochemical and electrophysiological parameters. Mol Neurobiol. 2023;60(7):4030–48.
30. Gulisano W, Maugeri D, Baltrons MA, Fa M, Amato A, Palmeri A, et al. Role of amyloid-beta and tau proteins in Alzheimer's disease: confuting the amyloid cascade. J Alzheimers Dis. 2018;64(s1):S611–31.
31. Grochowska KM, Gomes GM, Raman R, Kaushik R, Sosulina L, Kaneko H, et al. Jacob-induced transcriptional inactivation of CREB promotes Aβ-induced synapse loss in Alzheimer's disease. EMBO J. 2023;42(4):e112453.
32. Heppner FL, Ransohoff RM, Becher B. Immune attack: the role of inflammation in Alzheimer disease. Nat Rev Neurosci. 2015;16(6):358–72.
33. Wang WY, Tan MS, Yu JT, Tan L. Role of pro-inflammatory cytokines released from microglia in Alzheimer's disease. Ann Transl Med. 2015;3(10):136.
34. Strasser B, Berger K, Fuchs D. Effects of a caloric restriction weight loss diet on tryptophan metabolism and inflammatory biomarkers in overweight adults. Eur J Nutr. 2015;54(1):101–7.
35. Denninger JK, Smith BM, Kirby ED: Novel object recognition and object location behavioral testing in mice on a budget. J Vis Exp, 141 (2018)
36. Souza LC, Filho CB, Goes AT, Fabbro LD, de Gomes MG, Savegnago L, et al. Neuroprotective effect of physical exercise in a mouse model of Alzheimer's disease induced by beta-amyloid(1) (-)(4)(0) peptide. Neurotox Res. 2013;24(2):148–63.
37. Rahman A, Rao MS, Khan KM. Intraventricular infusion of quinolinic acid impairs spatial learning and memory in young rats: a novel mechanism of lead-induced neurotoxicity. J Neuroinflammation. 2018;15(1):263.
38. Sharma VK, Singh TG, Prabhakar NK, Mannan A. Kynurenine metabolism and Alzheimer's disease: the potential targets and approaches. Neurochem Res. 2022;47(6):1459–76.
39. Raich I, Lillo J, Rebassa JB, Capo T, Cordomi A, Reyes-Resina I, et al. Dual role of NMDAR containing NR2A and NR2B subunits in Alzheimer's disease. Int J Mol Sci. 2024. https://doi.org/10.3390/ijms25094757.
40. Bading H. Therapeutic targeting of the pathological triad of extrasynaptic NMDA receptor signaling in neurodegenerations. J Exp Med. 2017;214(3):569–78.
41. Lugo-Huitron R, Blanco-Ayala T, Ugalde-Muniz P, Carrillo-Mora P, Pedraza-Chaverri J, Silva-Adaya D, et al. On the antioxidant properties of kynurenic acid: free radical scavenging activity and inhibition of oxidative stress. Neurotoxicol Teratol. 2011;33(5):538–47.
42. Zwilling D, Huang SY, Sathyasaikumar KV, Notarangelo FM, Guidetti P, Wu HQ, et al. Kynurenine 3-monooxygenase inhibition in blood ameliorates neurodegeneration. Cell. 2011;145(6):863–74.
43. Wirthgen E, Hoeflich A, Rebl A, Gunther J. Kynurenic acid: the Janus-faced role of an immunomodulatory tryptophan metabolite and its link to pathological conditions. Front Immunol. 2017;8:1957.
44. Dos Santos NCL, Malta SM, Franco RR, Silva HCG, Silva MH, Rodrigues TS, et al. Antioxidant and anti-Alzheimer's potential of Tetragonisca angustula (Jatai) stingless bee pollen. Sci Rep. 2024;14(1):308.
45. El-Seedi HR, Eid N, Abd El-Wahed AA, Rateb ME, Afifi HS, Algethami AF, et al. Honey bee products: preclinical and clinical studies of their anti-inflammatory and immunomodulatory properties. Front Nutr. 2021;8:761267.
46. Tang YP, Shimizu E, Dube GR, Rampon C, Kerchner GA, Zhuo M, et al. Genetic enhancement of learning and memory in mice. Nature. 1999;401(6748):63–9.
47. Wang M, Yang Y, Wang CJ, Gamo NJ, Jin LE, Mazer JA, et al. NMDA receptors subserve persistent neuronal firing during working memory in dorsolateral prefrontal cortex. Neuron. 2013;77(4):736–49.
48. Liu Y, Fang S, Liu LM, Zhu Y, Li CR, Chen K, et al. Hearing loss is an early biomarker in APP/PS1 Alzheimer's disease mice. Neurosci Lett. 2020;717:134705.
49. Ordonez-Gutierrez L, Fernandez-Perez I, Herrera JL, Anton M, Benito-Cuesta I, Wandosell F. AbetaPP/PS1 transgenic mice show sex differences in the cerebellum associated with aging. J Alzheimers Dis. 2016;54(2):645–56.
50. Naatanen R, Paavilainen P, Alho K, Reinikainen K, Sams M. The mismatch negativity to intensity changes in an auditory stimulus sequence. Electroencephalogr Clin Neurophysiol. 1987;40(Suppl):125–31.
51. Biasibetti R, Almeida Dos Santos JP, Rodrigues L, Wartchow KM, Suardi LZ, Nardin P, et al. Hippocampal changes in STZ-model of Alzheimer's disease are dependent on sex. Behav Brain Res. 2017;316:205–14.
52. Bao J, Mahaman YAR, Liu R, Wang JZ, Zhang Z, Zhang B, et al. Sex differences in the cognitive and hippocampal effects of streptozotocin in an animal model of sporadic AD. Front Aging Neurosci. 2017;9:347.

Publisher's Note Springer Nature remains neutral with regard to jurisdictional claims in published maps and institutional affiliations.